



TM-936-A
1183.000

The Influence of Target Thickness and Backstop Material on
Proton-Produced Neutron Beams for Radiotherapy*

MIGUEL AWSCHALOM, IVAN ROSENBERG
Fermilab Cancer Therapy Facility, Batavia, Illinois 60510

AND

T. Y. KUO, J. L. TOM
The Cyclotron Corporation, Berkeley, California 94710

December 1979

*This work was supported in part by NCI Grant #2P01 CA 18081

The Influence of Target Thickness and Backstop Material on
Proton-Produced Neutron Beams for Radiotherapy.

INTRODUCTION

In the design of a neutron beam generator suitable for radiation therapy, it is desirable to achieve both a high dose rate and good penetration while keeping the activation of the target region and the skin entrance dose as small as possible. In a previous paper¹, it was argued that these requirements could be achieved using high energy proton beams incident on beryllium targets which do not completely absorb the incident proton energy. The improvement would be due both to the fact that the neutrons produced by the lower energy protons, as they slow down in the target, have a deteriorating effect on the overall quality of the beam, and that a higher proton beam current could safely be used, by dissipating the lower energy part of the beam power in a more suitable material such as water and carbon. Beryllium targets of different thicknesses were therefore made for interchangeable mounting in target holders that are easily replaceable on the end of the vacuum beam line. The measurements were carried out at the Cyclotron Corporation² to test these concepts.

EXPERIMENTAL ARRANGEMENTS

A CP42 cyclotron built by TCC was used in the experiment. A horizontal beam was extracted from the cyclotron and directed to a water-cooled target assembly (Fig. 1), designed for easy access and interchangeability of targets.

The proton energy was 41.9 ± 0.3 MeV. This energy was determined by a range-energy method prior to the neutron beam measurements. A collimated proton beam was first allowed to pass through a 6 mm aluminum disk which maintained the vacuum of the beam line. After travelling a short distance in air, the proton beam was then further degraded by thin aluminum disks of various thicknesses. Finally, those protons which have a range greater than the total stopper thickness were collected by an end plate. Current signals were taken from the 6 mm Al disk and from the end plate. Efforts were made to eliminate error due to current fluctuation and interference between these two signals. The secondary emission current taken from the 6 mm Al plate was used as an on-line monitor. If the transmitted current is normalized with respect to the monitor current and plotted against the stopper thickness, one can obtain the fraction of the number of protons which have a range greater than the corresponding stopper thickness. The range of this particular proton beam can then be extracted.

- 3 -

The result is shown in Figure 2. The normalized ratios of $I(\text{end plate})/I(\text{total})$ are plotted against the thickness of aluminum stoppers. Along the abscissa the range-energy relationship is also indicated³. In the upper part of this figure, a differentiation of end plate current with respect to stopper thickness is also shown. The Gaussian shape distribution corresponds to the path length straggling of the proton beam of a given energy. The centroid of this distribution coincides with the 50% point of the ratio plot which occurred at 7.87 mm, or at proton energy of 41.9 MeV. The $1/2 \delta R$ value (path length straggling) was found to be about 0.124 mm compared to a predicted value of 0.108 mm if 1% FWHM energy resolution is assumed.

The neutron beam was shielded and collimated by a large Benelex shield from an isocentric gantry under construction. The opening in the Benelex shield defined a $10 \times 10 \text{ cm}^2$ field at 125 cm SSD (source-skin distance) and 90 cm source to collimator end distance (SDD), using the field definition to the 50% decrement lines at the surface⁴. The phantoms used for the measurements were positioned in front of the collimator using a transit. The A-150 TE plastic⁵ block used for build-up measurements was placed 35 cm from the collimator end. The TE-liquid⁶ phantom used for the other measurements was placed at 34 cm from the collimator end, while the position

of the interchangeable target was found to be at 87.6 cm SDD, because of the different design from the standard target holder. This gave an SSD of 121.6 cm and a nominal field size at the surface of the tank of $10.2 \times 10.2 \text{ cm}^2$ (Fig. 3). The phantom had dimensions of $30 \times 30 \times 30 \text{ cm}^3$ and a front perspex window of thickness 0.51 mm. It was filled with TE fluid⁶ of density $1.071 \pm 0.016 \text{ g cm}^{-3}$. Three air-filled ionization chambers were used for different depths.

- (a) An extrapolation chamber, made of A-150 TE plastic, EG&G model EIC, having an outer diameter of 2.54 cm and a window of 2.9 mg cm^{-2} , was used for build-up measurements inside a snugly fitting A-150 block of size $10 \times 10 \times 10 \text{ cm}^3$, and with A-150 discs of equal diameter as absorbers. This ionization chamber has an active volume diameter of 1 cm, and it was adjusted to have a plate-to-plate spacing of 2.25 mm.
- (b) A 0.1 cc, EG&G model IC-18, A-150 plastic thimble chamber of outside diameter 0.8 cm and 0.16 cm wall thickness was used in the TE solution phantom for depths from just beyond maximum build-up to about 10 cm deep.
- (c) A 1.0 cc, EG&G model IC-17, A-150 plastic spherical chamber of outside diameter 2.3 cm and 0.5 cm wall thickness was used for depth of 10 cm and deeper in

- 5 -

the phantom. This chamber had been calibrated in terms of ^{60}Co exposure in air using the Fermilab ^{137}Cs calibrator, traceable to NBS⁷.

All these chambers were connected to a Keithley 616 digital electrometer, via a low noise coaxial cable. The polarizing HV was supplied by batteries, +300 V for the IC-18 chamber and +600 V for the others. The leakage currents observed for the combination of chamber, cable and electrometer were of the order of 1×10^{-14} A for all three chambers. Only positive collection voltages were used on all three chambers, adequate for more than 99% collection efficiency. Preliminary measurements with the extrapolation chamber at both +600 V and -600 V using the p(66)Be(49)^{*} neutron beam at Fermilab showed that a correction factor of about 0.99 should be applied to the positive voltage collected charge using the thinnest window (2.9 mg cm^{-2}), this correction increasing to almost 1.0 at maximum build-up thickness and beyond.

The charged particle current on target was measured with a Brookhaven Instrument Corporation Model 1000C current indicator and digital integrator. The target was biased with a DC voltage of 45 Volts to an electron suppression ring as

* This notation, used in reference 4, means that the neutron beam was produced by protons incident on a Be-target. The target thickness is such that 66 MeV protons traversing the target without making nuclear collisions lose 49 MeV.

shown on Figure 1. A thick collimator ring was placed upstream of the electron suppression ring and target to prevent any stray cyclotron beam from striking the target.

METHOD OF MEASUREMENTS

The extrapolation chamber was used to measure the entrance dose, bracket the position of the broad maximum expected to be at about 0.8 cm deep⁸, estimate the depth at which the rise of the build-up reached 90% of maximum and determine the percent depth dose at 1.4 g cm^{-2} . This last value was then used as a normalization for measurements obtained with the thimble ionization chamber (IC-18) at 1.31 cm deep ($= 1.4 \text{ g cm}^{-2}$). The ratio of these measurements to those at 9.75 cm deep with the same chamber were then used to obtain the percent depth dose at this depth. This percent depth dose was in turn used to normalize the ratio obtained by the large spherical chamber (IC-17), at various depths and to obtain an interpolated value for the depth of the 50% depth dose. All depths were defined at the center of the chambers, with coincidence of the two chambers at 9.75 cm deep. This depth was ensured by using precision stainless steel gauge bars to set the distance from the inner face of the filled phantom. The intercomparison between the extrapolation and thimble chambers was done at 1.4 g cm^{-2} , well beyond the depth of maximum dose, in order to use the latter chamber only in a region where the normalized neutron and charged particle spectra were changing slowly, with depth, thus ensuring proportionality between measured ionization and dose.

- 7 -

UNCERTAINTIES

Because of the way the measurements with one chamber affect the normalization of data taken with another chamber, the uncertainties in the data have to be transferred from one set of measurements to the next one. For the extrapolation chamber, the ratios obtained have the following uncertainties:

- 0.5% precision of measurement,
- 0.3% precision of positioning (2 mm in 125 cm), and
- 1.0% systematic uncertainty due to the above mentioned polarity effect.

This gives a 1.6% uncertainty over all.

Similarly, for the 0.1 cc thimble chamber:

- 0.5% precision,
- 0.3% position (2 mm in 125 cm), and
- 0.5% uncertainty in the assumption that the %DD at 1.3 cm deep is the same for all target configurations, i.e., $98.5 \pm 0.5\%$ of D_{\max} .

These, added in quadrature to the 1.6% carried over from the extrapolation chamber, give 1.8%.

At the greater depths, the 1.0 cc IC-17 chamber adds 0.5% for precision and 0.3% for positioning, for a total of $\pm 1.9\%$

- 8 -

uncertainty in %DD at depth. This overall uncertainty translates to ± 2 mm in the value of the depth of the 50 depth dose.

The measurements of the IC-17 chamber at 9.75 cm deep were also used to obtain the total dose in rad/mC, corrected for 125 cm SSD, and the %DD at 9.75 cm was used to transfer the dose to the maximum dose point. To the 1.9% uncertainty due to precision, the dose values have added uncertainties due to accuracy^{9, 10} for an overall uncertainty of 7.7 - 9.0%. These error limits cover uncertainties in chamber calibration in a ⁶⁰Co beam and uncertainties in neutron beam conversion factors in addition to the previously discussed precision limits.

RESULTS

In all, four target thicknesses were investigated:

- "A" a pure beryllium target, 1.21 cm thick, which would stop 42 MeV protons completely;
- "B" syntered material¹¹, HP-10, 0.81 cm thick, which would remove 22.6 MeV from a 42 MeV proton beam;
- "C" syntered material, HP-10, 0.60 cm thick, which would remove 15.3 MeV from a 42 MeV proton beam;
- "D" syntered material, HP-10, 0.35 cm thick, which would remove 8.3 MeV from a 42 MeV proton beam.

- 9 -

First, build-up curves were obtained for targets "A" and "D", the extremes of the range, as well as for target "A" with filtration as proposed for the M. D. Anderson beam¹²:

2.1 cm (1.9 g cm^{-2}) boron loaded (5%) polyethylene immediately after the target and a further layer of polyethylene, shaped as a flattening filter, at the downstream end of the collimator, having maximum thickness of 3.15 cm (2.9 g cm^{-2}).

Figure 4 shows the results of the measurements, all normalized to 100% at dose maximum. There is surprisingly little difference in the curves for the three target configurations: the entrance dose varies from 49 (± 1)% of maximum for the filtered "A" target to 52 (± 1)% for the unfiltered "A" target to 54 (± 1)% for "D". This last result is contrary to expectations for a thin target¹ and will be discussed more later. All three curves show that the build-up rises to 90% of maximum well within 0.25 g cm^{-2} from the surface and that the maximum lies between 0.6 and 1.0 g cm^{-2} , with some indication that it shifts slightly deeper for the thinner target. The points taken at 1.4 g cm^{-2} all fall close together at 98.5 (± 0.4)% of maximum dose. As these targets spanned the whole range of thicknesses of interest, it was assumed that the dose at 1.4 g cm^{-2} (or 1.31 cm of TE fluid) was 98.5% of maximum for all other target configurations used.

- 10 -

Figure 5 shows the variation of the depth of half-maximum dose with target thickness and filtration. The depths are expressed in cm of TE liquid ($\rho = 1.07 \text{ g cm}^{-3}$) for a SSD of 125 cm and a field size of $10.2 \times 10.2 \text{ cm}^2$ at the surface. Two filters were used: #1 a polyethylene block with 5% boron, 6 cm thick (5.2 g cm^{-2}), and #2 a plain polyethylene block, 6 cm thick (5.5 g cm^{-2}), both immediately after the target, with no flattening filter. As can be seen, there is an initial improvement in penetration as the target is made thinner, but then there seems to be an evening out or even a reversal of the trend for progressively thinner targets. This is again contrary to expectations¹. It can also be noted that the use of a filter greatly improves the penetration, and that the amount of filtering does influence the quality of the beam.

Finally, in figure 6 the relative dose per unit proton charge of the different target configurations are presented, with and without filtration. The normalization point is taken as the yield of the full thickness target "A" without filtration, which was found to be $27.9 \pm 2.5 \text{ rad/mC}$ (or $1.67 \pm 0.15 \text{ rad min}^{-1} \mu\text{A}^{-1}$) at D_{max} for 125 cm SSD, and a $10.2 \times 10.2 \text{ cm}^2$ beam. The

dotted line is the predicted relative dose per unit charge given by the expression

$$D_T/D_\infty = 1 - \left(\frac{E_i - e_t}{E_i} \right)^\beta \quad (1)$$

where E_i is the incident energy of the protons, e_t is the proton ionization energy lost in the target, and a value for β of 3.2 was used¹.

DISCUSSION

The build-up curves shown in Figure 4 can be compared to other published results for the p-Be reaction at 26 MeV¹³, 35 MeV⁸ and 42 MeV¹⁴ incident proton energy. Although the expected increase with energy of the depth of maximum build-up is apparent, the value of the percent dose at the entrance shows no trend, being reportedly as low as 41% for 35 MeV⁸ and as high as 60% for both 26 MeV¹³ and 42 MeV¹⁴. In particular, there is poor agreement between the present result and the most directly comparable one, at 42 MeV¹⁴, in relation to both the entrance dose and the depth of maximum build-up, as well as in the effects of filtration. These discrepancies may be due to differences in field size, collimator composition and measurement techniques.

The dose per unit proton charge and depth dose measurements obtained

using the thick target "A" can also be compared to similar measurements by other investigators, as shown in Table I. Although the dose rates listed in Table I are not strictly comparable, there is remarkable agreement, within the uncertainties of measurements, among the unfiltered thick target dose per unit proton charge. However, the dose attenuation caused by the hardening filters show some discrepancy between the present work and a previously published experiment⁸.

The agreement in the depth of the 50% depth dose, for total (n + γ) dose measurements, is good for the unfiltered beams, but poor, again, for the filtered ones. Both results seem to indicate different filter effects in the two experiments, with the filters used in the present work being less effective. As the nominal thicknesses of the polyethylene blocks were the same in both experiments, these differences are hard to explain even taking into account typical variations in polyethylene densities (0.92 - 0.96 g/cm³).

The striking outcome of the present work, however, is provided by the discrepancies from expected behavior as progressively thinner targets are investigated. These discrepancies are:

- (a) The entrance dose was expected to diminish as a fraction of D_{\max} as the targets become thinner.

The results in Fig. 4 show an opposite trend.

- (b) The penetration of the neutron beam was expected to increase monotonically as the targets became thinner. The results in Fig. 5 show this to be true at first, but that with even thinner targets, this increase is halted or even reversed.
- (c) The relative dose rate from different thickness targets at constant incident proton energy can be predicted from expression (1), if the value of β is known. This value can either be derived from the relative dose per unit incident charge from "thick" targets at different incident energies from the expression

$$\dot{D}(E_i) \propto E_i^\beta \quad (2)$$

or from actual measurements using thin and thick targets at constant incident energy. Values of β using expression (2) can be obtained from published results, ranging from 2.2¹⁶ to 2.8⁸ to 2.9¹⁵, while a value of 3.2 was derived in the previous paper¹ from expression (1) using data in reference 16. This last value, which predicts the largest relative dose rate for thinner targets, has been used in plotting the theoretical curve shown in Fig. 6. It can be seen that the measured dose rates are in excess

- 14 -

of those predicted from this curve. To fit these results, a larger and variable value for β would be required.

- (d) Although it was not discussed in the previous paper¹, a prediction can be made on the effect of filtration on the beams produced by progressively thinner targets.

It is shown in the appendix that in the limiting case of a very thin target, the penetration with filtration should improve less markedly than for the thick target. For intermediate target thicknesses there should be a progressive effect in that direction. The measurements obtained with filter #1 for the thick "A" target and the thinnest "D" target, as well as those with filter #2 for "A" and "C" targets, on the other hand, show an equal or even larger improvement with the thinner targets.

All of the above discrepancies could be explained if, in spite of the progressively thinner targets, a significant fraction of the neutron dose were produced by the protons emerging from the Be-target, since all of the arguments used in the predictions assumed that this contribution did not exist. In fact, the protons emerging from the thin beryllium

- 15 -

targets must interact and be stopped by the 2 mm thick copper backstop of the target. These targets were designed to fit a pre-existing assembly system, with provisions for easy handling and replacement. The main purpose of a copper backing was to provide a good vacuum seal in case the beryllium target developed a crack.

To check on the possibility that the results were being vitiated by the influence of these backstops, rough estimates were made of the dose contribution to D_{\max} from neutrons generated by the protons emerging from the thin targets and stopped by the copper backstop. These estimates and their effect on the results are shown in Table II. In these calculations, all neutrons created in the copper are assumed to have an evaporation spectrum. This assumption underestimates the beam energy and neutron flux in the direction of the incident proton beam. The corrections are derived using data from Tai et. al.¹⁷ Furthermore, it is assumed that the dose contribution from these neutrons would be unattenuated at D_{\max} , and that it would subsequently diminish at depth following the attenuation curve for approximately a 2.0 MeV neutron beam¹⁸. Thus, for example, the "corrected" relative doses in column 9 are obtained by subtracting the values in column 5 from the observed doses per unit charge in column 6, then normalizing to the corresponding thick target values. The "corrected" depths for

- 16 -

half-maximum dose shown in column 11 are arrived at by subtracting the surviving contribution of this "spurious" dose at each measured depth, as well as at D_{\max} , and then repeating the interpolation process from the "corrected" percent depth doses.

It is encouraging that this admittedly rough estimate of the effect of the copper backstop improves the agreement between the predicted and "corrected" relative doses per unit charge more significantly, restores a monotonic trend to the "corrected" depth of the 50% depth dose for progressively thinner targets. These calculations therefore bear out the hypothesis that the effect of the copper backstop is not negligible and can influence the results, sometimes dramatically.

CONCLUSIONS

Although the results presented in this paper do not completely support the predictions on which the original concept was based, namely the use of thin targets to improve the performance of clinical neutron generators¹, they do not disprove them either. The inconclusiveness of these results is due to the unwise use of a thick copper backstop which defeated the purpose of using thin beryllium targets. A different target assembly should be designed, perhaps

- 17 -

using a combination of water for cooling and carbon (graphite) for further energy degradation of the protons as the major backstop.¹ Measurements should then be repeated under these conditions before any final judgement is passed on the basic concepts.

ACKNOWLEDGEMENTS

The authors wish to thank George Hendry for his valuable comments and numerous suggestions throughout the length of this project.

The generous and invaluable help of Fred Ramsey in running the cyclotron during the gathering of these results is gratefully acknowledged.

Two of the authors (Miguel Awschalom and Ivan Rosenberg) want to thank Dr. James W. Blue and Dr. William Robert of the Great Lakes Neutron Therapy Association, NASA, Cleveland, Ohio, for the suggestion of using water plus graphite energy absorbers in lieu of a pure water absorber downstream from the Be-targets.

REFERENCES

1. M. Awschalom, I. Rosenberg, preceding paper in Med. Phys.
2. Berkeley, California 94710.
3. Janni, J. F. Range Energy Calculations, USAF publ. AFWL-TR-65-150, September 1966.
4. American Association of Physicists in Medicine, Task Group 18, "Protocol for Neutron Beam Dosimetry", section 7.1.
5. Ibid., Table I.
6. N. A. Frigerio, R. F. Coley, and M. J. Sampson, Table II. Phys. Med. Biol. 17, 792 (1972).
7. M. Awschalom, I. Rosenberg, Fermilab Technical Report, TM-834, December 1978.
8. W. M. Quam, S. W. Johnson, G. O. Hendry, J. L. Tom, P. H. Heintz, R. B. Theus, Phys. Med. Biol. 23, 47 (1978).
9. Ibid.⁽⁴⁾, section 5.1.1, paragraph h.
10. Ibid.⁽⁴⁾, section 5.1.2, paragraph g.
11. Kawecky Berylco Industries, Inc. New York, New York.
12. P. R. Almond, V. A. Otte, W. H. Grant, J. Smathers, R. Graves, IEEE Trans. Nucl. Sci. NS-26, 1724, (1979).
13. D. T. Goodhead, R. J. Berry, D. A. Bance, P. Gray, B. Stedeford, Phys. Med. Biol., 23, 144 (1978).
14. B. J. Mijnheer, J. Zoetelief, J. J. Broerse, Br. J. Radiol. 51, 122 (1978).
15. F. M. Waterman, F. T. Kuchnir, L. S. Skaggs, R. T. Kouzes, W. H. Moore, Med. Phys. 6, 432 (1979).
16. H. I. Amols, J. F. Dicello, M. Awschalom, L. Coulson, S. W. Johnson, R. B. Theus, Med. Phys. 4, 486 (1977).
17. Y. K. Tai, G. P. Millburn, S. N. Kaplan, B. J. Moyer, Phys. Rev. 109, 2086 (1958).
18. N.B.S. Handbook 63, B.P.O., Washington, D.C. 1957.
19. R. S. Caswell, J. J. Coyne, M. L. Randolph, submitted for publication.

20. C. J. Batty, B. E. Bonner, A. I. Kilvington, C. Tschalar, L. E. Williams, Nucl. Instr. & Meth. 68, 273 (1969).
21. R. G. Graves, J. B. Smathers, P. R. Almond, W. H. Grant, V. A. Otte, Med. Phys. 6, 123 (1979).
22. R. G. Alsmiller, J. Barish, Health Phys. 33, 98 (1977).
23. D. J. Hughes, R. B. Schwartz, BNL-325, 2nd ed. July 1, 1958.

TABLE I

COMPARISON OF DOSE RATE AND DEPTH DOSE RESULTS FOR THICK 42 MeV TARGETS

Investigator	Unfiltered Beam		Beam With 6 cm Filter		NOTES
	Dose Rate $\text{rad min}^{-1}\mu\text{A}^{-1}$	Depth of 50%DD cm (f)	Dose Rate $\text{rad min}^{-1}\mu\text{A}^{-1}$	Depth of 50%DD cm (f)	
Present work	$1.67 \pm .15$	11.6 ± 0.2	$1.07 \pm .09$ $1.00 \pm .09$	12.6 ± 0.2 12.9 ± 0.2	Filter #1 (a) Filter #2 (a)
Quam et al. ⁸	$1.73 \pm .12$	11.7 ± 0.2	$0.95 \pm .07$	13.7 ± 0.2	(b)
Waterman et al. ¹⁵	$1.59 \pm .10$	—	—	—	(c)
Mijnheer et al. ¹⁴	—	11.2	—	12.6	(d)
Almond et al. ¹²	—	—	0.70	13.2	(e)

Notes: (a) Total (n+ γ) dose rate at D_{max} , $10.2 \times 10.2 \text{ cm}^2$ beam at 125 cm SSD.

(b) Total (n+ γ) kerma-rate in air (interpolated), $10.8 \times 10.8 \text{ cm}^2$ beam at 125 cm SSD. Polyethylene filter.

(c) Total (n+ γ) kerma-rate in air (interpolated) uncollimated beam at 125 cm SSD.

(d) Neutrons only depth dose, 17 cm diameter circle at 125 cm SSD. Nylon filter (1.15 g cm^{-3}).

(e) Total (n+ γ) kerma-rate in air, $10 \times 10 \text{ cm}^2$ beam at 125 cm SSD. 41 MeV protons filtered as described in text and in Ref. 12.

(f) Measured in TE liquid ($\rho = 1.07 \text{ g cm}^{-3}$), except for Ref. 14, where water depths have been corrected for density only.

TABLE II

Influence of Copper Backing on Dose per Unit Charge and Depth Dose for Unfiltered Thin Targets

1 Target	2 e_t MeV	3 Residual Energy MeV	4 Copper Contribution		6 Observed (Total Dose per Unit chg. rad/mC (f))	7 Observed Relative Dose per Unit Charge	8 Predicted Relative Dose per Unit Charge (g)	9 "Corrected" Relative Dose per Unit Charge	10 Observed Depth of $D_{max}/2$ cm	11 "Corrected" Depth of $D_{max}/2$ cm
			Neutrons $cm^{-2}\mu C^{-1}$ (a)	Dose at D_{max} rad/mC (b)						
A	42	0	0	0	27.9 ± 2.5	1.00	1.000	1.00	11.6 ± 0.2	11.6
B	22.8	19.2	$1.0 \cdot 10^5$ (c)	0.38	25.7 ± 2.3	0.92 ± 0.025	0.916	0.91	12.2 ± 0.2	12.3
C	15.3	26.7	$2.8 \cdot 10^5$ (d)	1.1	21.2 ± 1.9	0.78 ± 0.021	0.765	0.74	12.3 ± 0.2	12.6
D	8.3	33.7	$4.9 \cdot 10^5$ (e)	1.9	16.4 ± 1.5	0.59 ± 0.016	0.506	0.52	12.0 ± 0.2	12.8

NOTES:

- (a) At 125 cm SSD.
 (b) Assuming dose = kerma and kerma = $0.38 \cdot 10^8$ rad cm^2 (Ref. 19).
 (c) 0 - 18 MeV data extrapolated to 19 MeV (Ref. 17).
 (d) Interpolated using $N(E_p) = 2.03 \cdot 10^{-3} E_p^{2.4}$ Ref. 17).
 (e) 0 - 32 MeV data extrapolated to 34 MeV (Ref. 17).
 (f) At D_{max} for 10.2×10.2 cm^2 field at 125 cm SSD.
 (g) From expression (1) with $\beta = 3.2$ (Ref. 1).

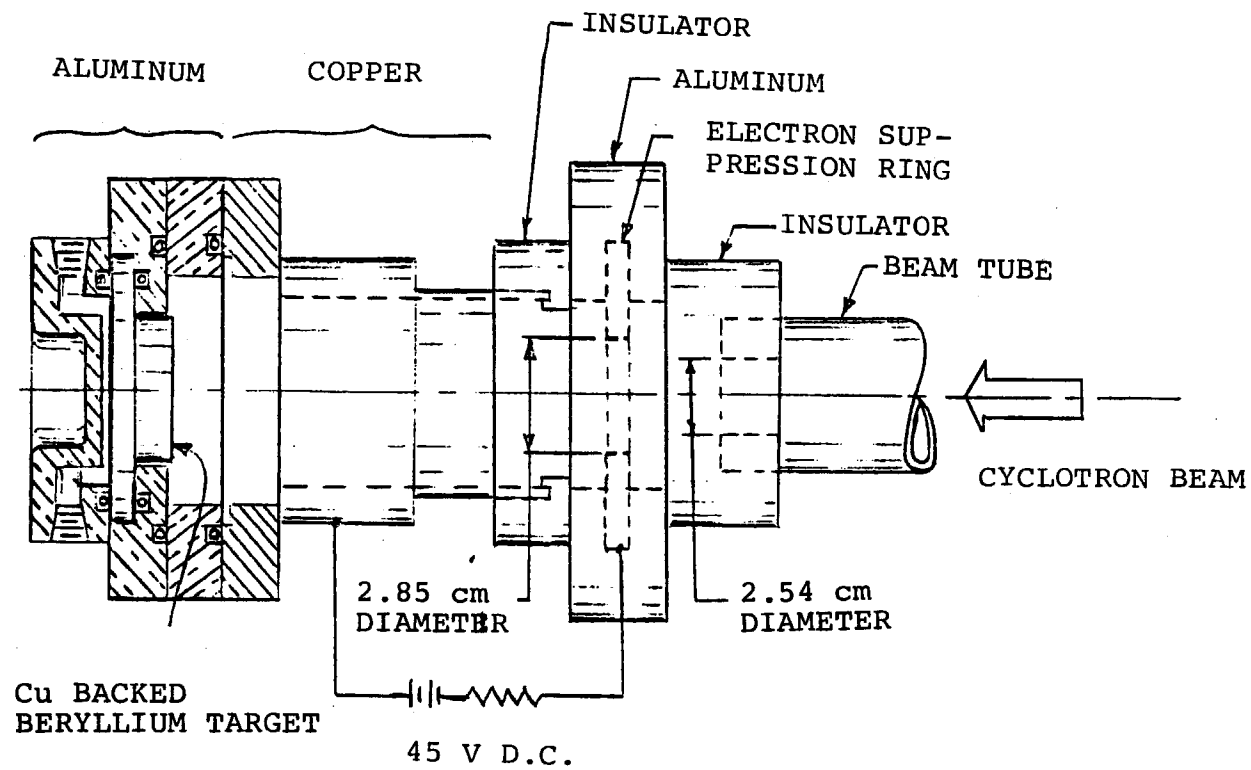


Fig. 1

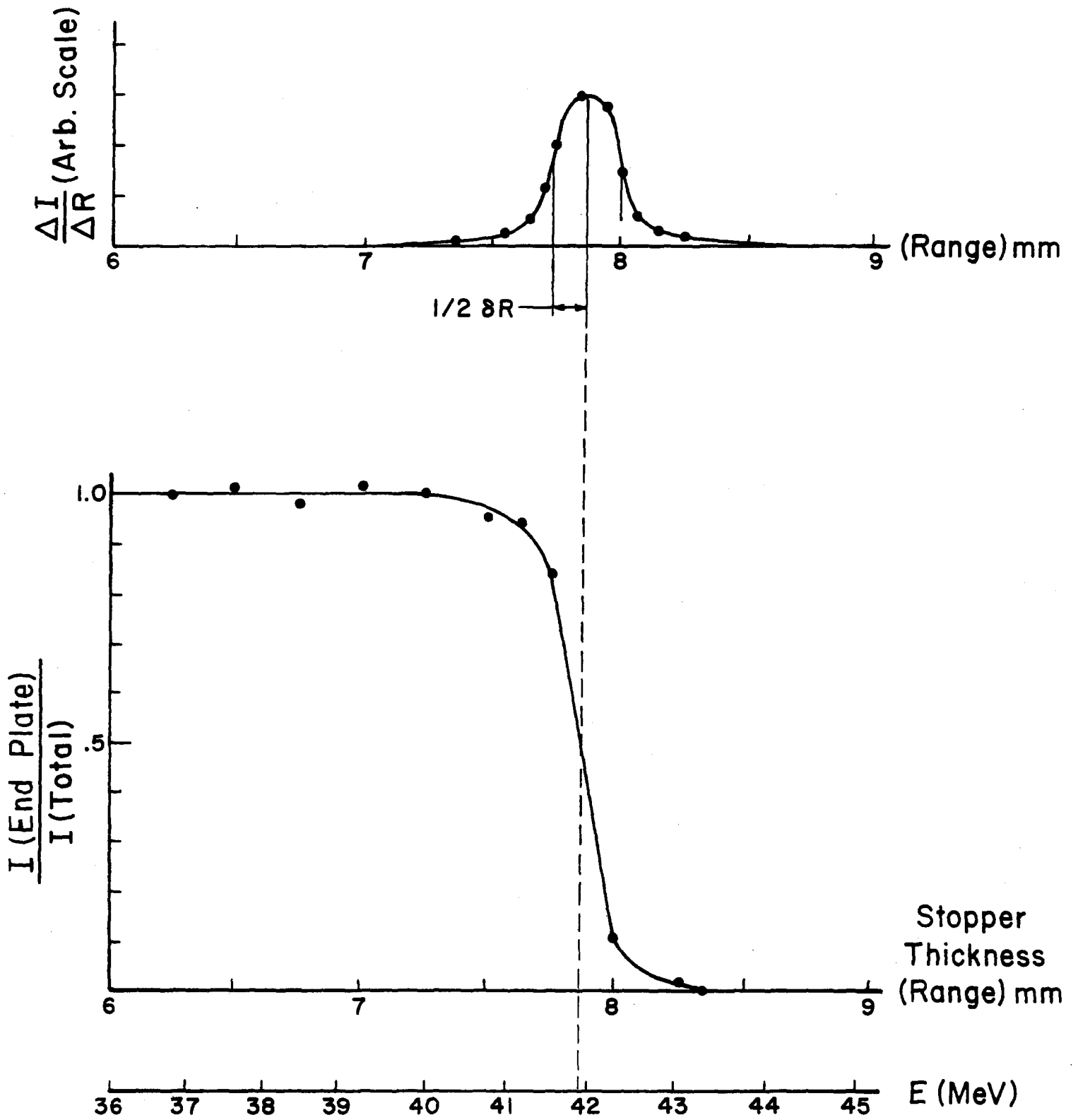
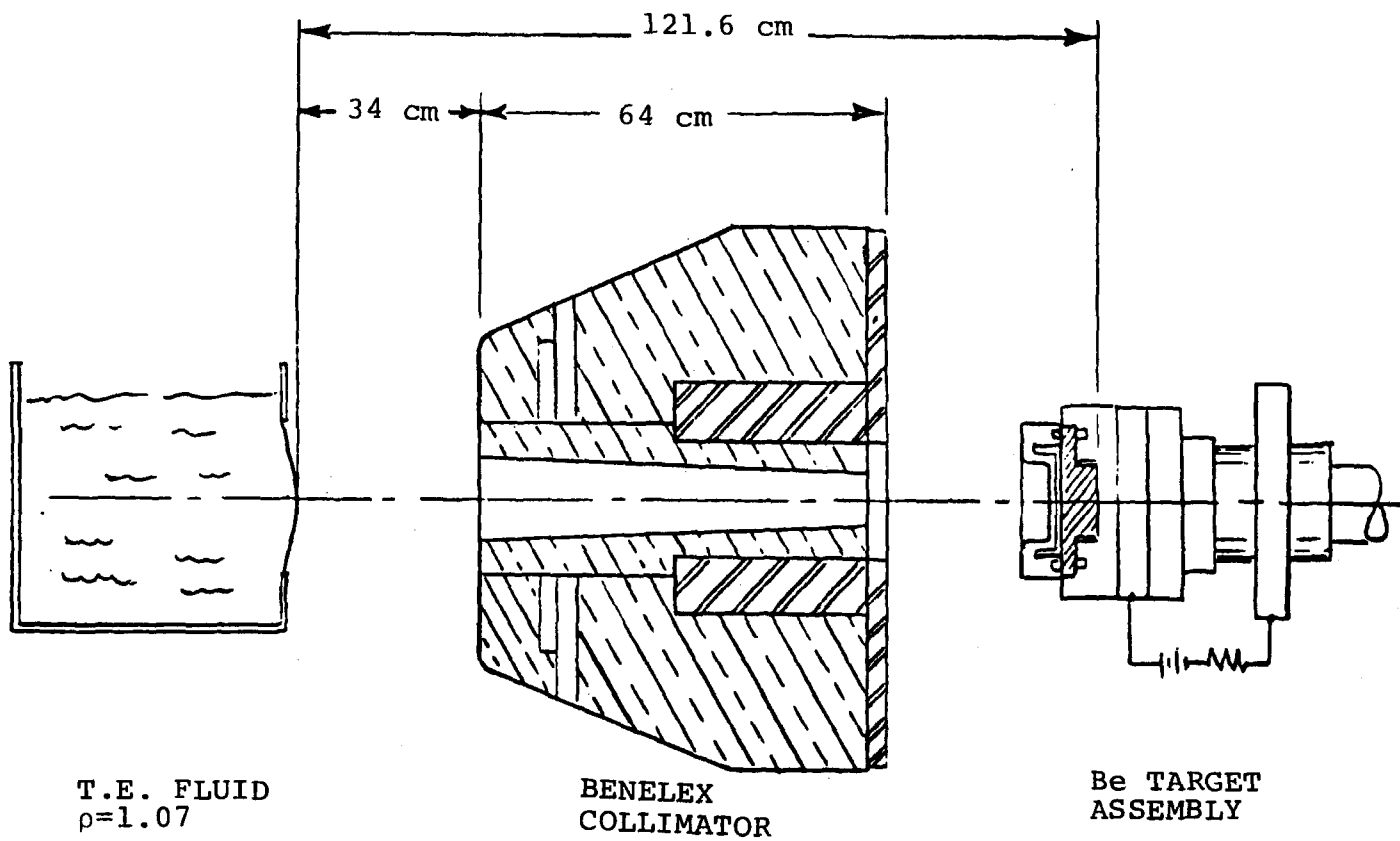


Fig. 2



T.E. FLUID
 $\rho = 1.07$

BENELEX
 COLLIMATOR

Be TARGET
 ASSEMBLY

Fig. 3

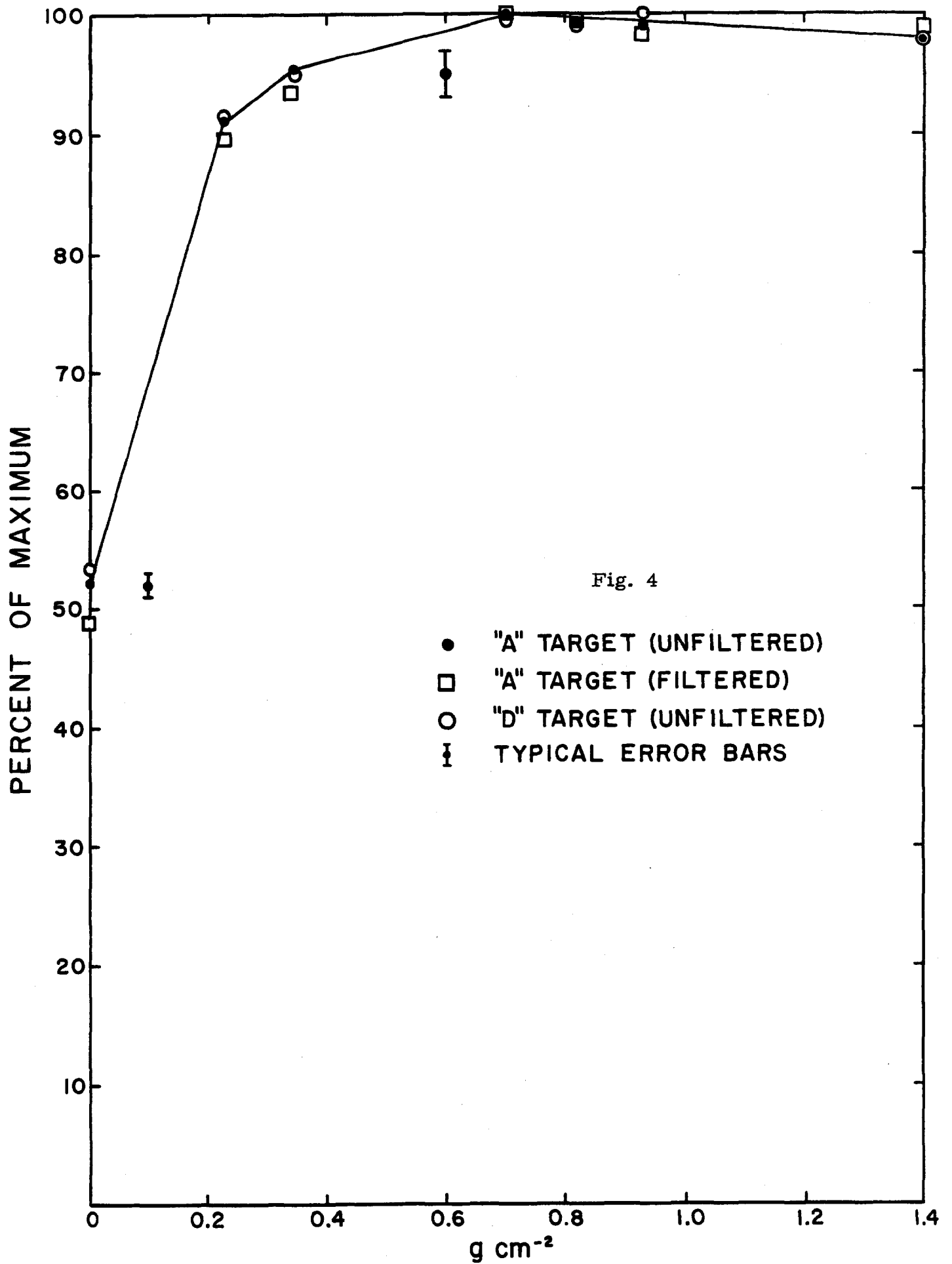


Fig. 4

- "A" TARGET (UNFILTERED)
- "A" TARGET (FILTERED)
- "D" TARGET (UNFILTERED)
- ⊥ TYPICAL ERROR BARS

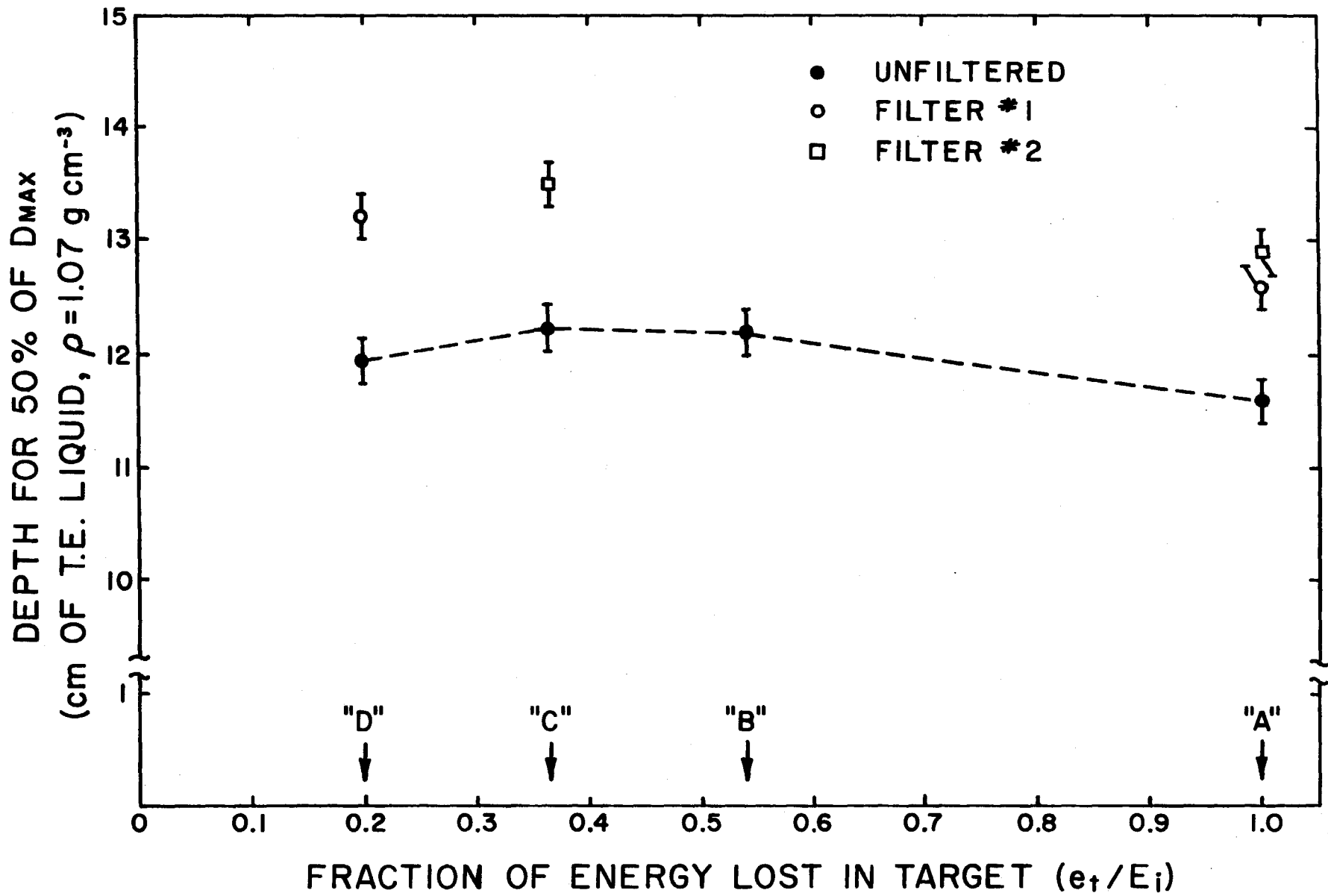


Fig. 5

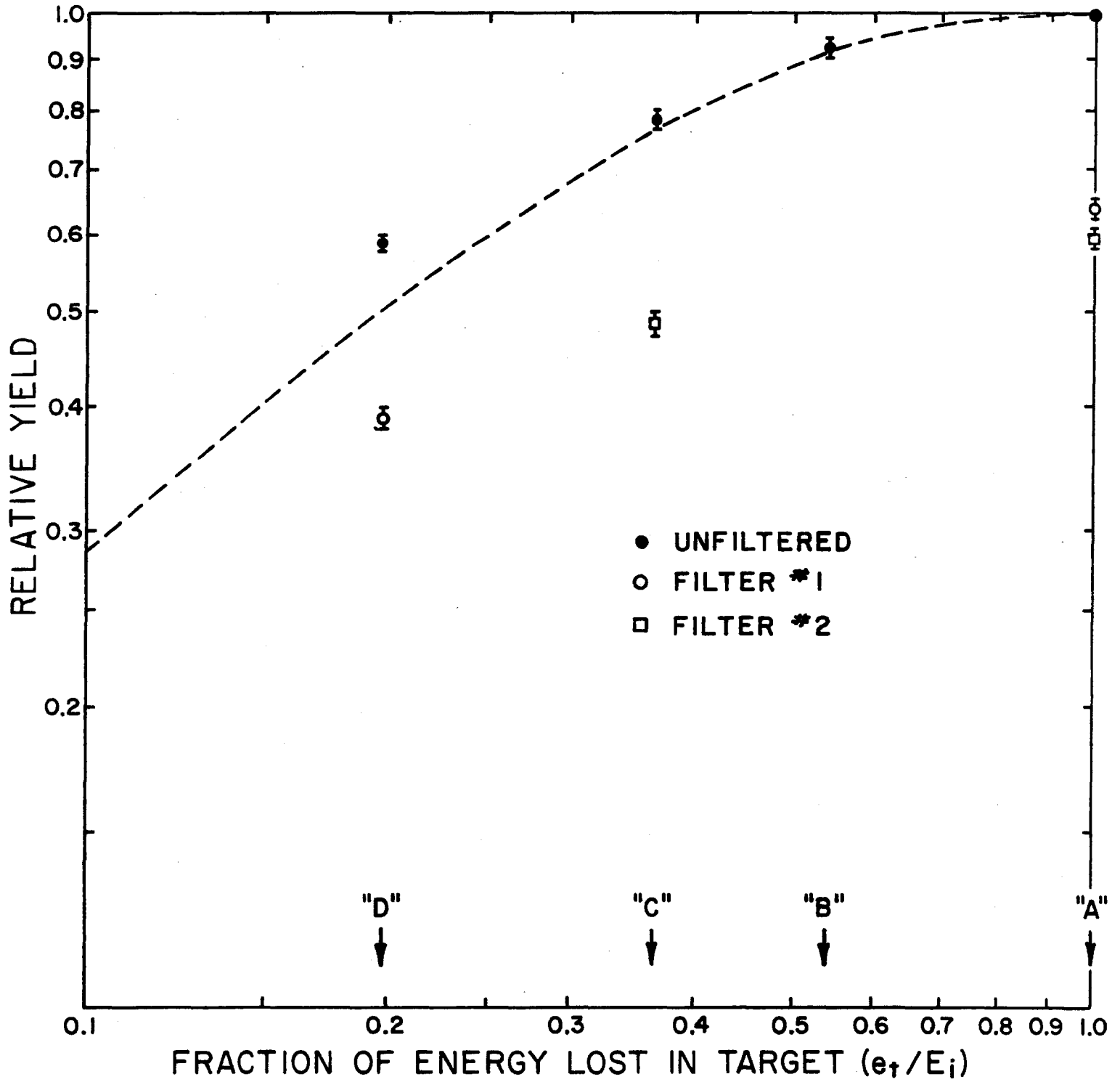


Fig. 6

APPENDIX

Effect of Hardening Filter on Thick and Thin Target Spectra.

In the limiting case of a very thin target, the resulting neutron energy spectrum would have quasi-elastic peaks at the high energy end, a low background (about one order of magnitude less than the quasi-elastic peak) at intermediate energies and an evaporation spectrum at low energies²⁰. The thick target, on the other hand, produces an energy independent distribution from near the maximum neutron energy to the 5 - 10 MeV region where the evaporation contribution begins to be significant.^{16, 21} On the other hand, the kerma for neutrons is a fast rising function of energy from zero up to a few MeV and then it continues to increase slowly.^{19, 22} Also, the total removal cross-section by the (n,p) reaction in tissue decreases monotonically with energy.^{1, 23} Combining these facts, it can be shown that a much larger fraction of the kerma is contributed by neutrons in the 10 - 35 MeV range in the thick target spectrum compared to the thin target one, and that the fraction contributed by the flux below 10 MeV is not dominant for either spectrum.

Now, the effect of the filter on the thick target spectrum consists of attenuating preferentially these low and intermediate energies.²⁰ However, in the thin target spectrum,

although the low energy (0 - 10 MeV) effect may be comparable to the thick target case, there is a much smaller intermediate energy flux to attenuate. Thus, the overall hardening effect of filtration should be less marked for the thin target than for the thick one, i.e., the improvement in the depth of the 50% depth dose due to filtration should be smaller for the thin target.